

ALPCAHUS: Subspace Clustering for Heteroscedastic Data

Javier Salazar Cavazos[✉], *Graduate Student Member, IEEE*,

Jeffrey A. Fessler[✉], *Fellow, IEEE*, and Laura Balzano[✉], *Senior Member, IEEE*

Electrical & Computer Engineering (ECE) Department, University of Michigan, Ann Arbor, Michigan, United States

Email: {javieresc, fessler, girasole}@umich.edu

Abstract—Principal component analysis (PCA) is a key tool in the field of data dimensionality reduction. Various methods have been proposed to extend PCA to the union of subspace (UoS) setting for clustering data that comes from multiple subspaces like K -Subspaces (KSS). However, some applications involve heterogeneous data that vary in quality due to noise characteristics associated with each data sample. Heteroscedastic methods aim to deal with such mixed data quality. This paper develops a heteroscedastic-based subspace clustering method, named ALPCAHUS, that can estimate the sample-wise noise variances and use this information to improve the estimate of the subspace bases associated with the low-rank structure of the data. This clustering algorithm builds on K -Subspaces (KSS) principles by extending the recently proposed heteroscedastic PCA method, named LR-ALPCAH, for clusters with heteroscedastic noise in the UoS setting. Simulations and real-data experiments show the effectiveness of accounting for data heteroscedasticity compared to existing clustering algorithms. Code available at <https://github.com/javieresc1/ALPCAHUS>.

Index Terms—Heteroscedastic data, heterogeneous data quality, subspace bases estimation, subspace clustering, union of subspace model, unsupervised learning.

I. INTRODUCTION

Many modern data science problems require learning an approximate signal subspace basis for some collection of data. This is important for downstream tasks involving subspace basis coefficients such as classification [1], regression [2], and compression [3]. Besides subspace learning, one may be interested in clustering data points that originate from multiple subspaces. Formally, subspace clustering, or union of subspace (UoS) modeling, is an unsupervised machine learning problem where the goal is to cluster unlabeled data and find the subspaces associated with each data cluster. When the cluster assignments are known, it is easy to find the subspaces, and vice versa. This problem becomes nontrivial when both components must be estimated [4]. This clustering problem has many applications, such as image segmentation [5], motion segmentation [6], image compression [7], and system identification [8].

Some applications involve heterogeneous data samples that vary in quality due in part to noise characteristics associated with each sample. A few examples of heteroscedastic datasets include environmental air quality data [9], astronomical spectral data [10], and biological sequencing data [11]. In heteroscedastic settings, the noisier data samples can significantly corrupt the basis estimates [12]. In turn, this corruption can worsen clustering performance as seen in Fig. 1. Popular clustering methods

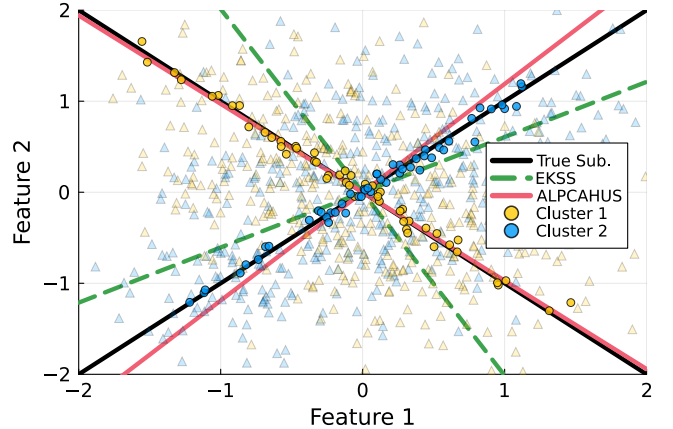


Fig. 1: Two 1D subspaces, colored blue and yellow, with data consisting of two noise groups shown with circle (low noise) and triangle (high noise) markers.

such as Sparse Subspace Clustering (SSC) [13], K -Subspaces (KSS) [14], and Subspace Clustering via Thresholding (TSC) [15], all implicitly assume that data quality is consistent. For example, in SSC, the method relies on the self-expressiveness property of data that uses other similar samples to estimate each single sample. From our experiments, we found that this implicit data quality assumption can degrade clustering quality for heteroscedastic data.

Because of these limitations, we developed a subspace clustering algorithm, inspired from KSS principles, that explicitly models noise variance terms, without assuming that data quality is known. The method adaptively clusters data while learning noise characteristics. See Fig. 1 for a visualization where Ensemble KSS (EKSS) [16] returns poor subspace bases estimates whereas our method found more accurate subspace bases and improved clustering quality.

We extend our previous work [17] by generalizing the LR-ALPCAH formulation to the UoS setting for clustering heteroscedastic data. The proposed approach achieved ~ 3 times lower clustering error than existing methods, and it achieved a relatively low clustering error even when very few high quality samples were available. The paper is divided into a few key sections. Sec. II introduces the heteroscedastic problem formulation for subspace clustering. Sec. III discusses related work in subspace clustering and reviews the heteroscedastic subspace algorithm LR-ALPCAH. Sec. IV introduces the

proposed subspace clustering method named ALPCAUS. Sec. V covers synthetic and real data experiments that illustrate the effectiveness of modeling heteroscedasticity in a clustering context. Finally, Sec. VI discusses some limitations of our method and possible extensions.

II. PROBLEM FORMULATION

Let K denote the number of subspaces that is either known beforehand or estimated using other methods. Before describing the general union of subspace model, the single subspace model under $K = 1$ is introduced.

A. Single Subspace Model ($K = 1$)

Let $\mathbf{y}_i \in \mathbb{R}^D$ denote the data samples for index $i \in \{1, \dots, N\}$, where D denotes the ambient dimension and N is the total number of samples. Let \mathbf{x}_i represent the low-dimensional data sample generated by $\mathbf{x}_i = \mathbf{U}\mathbf{z}_i$ where $\mathbf{U} \in \mathbb{R}^{D \times d}$ is an unknown basis for a subspace of dimension d and $\mathbf{z}_i \in \mathbb{R}^d$ are the corresponding basis coordinates. Then the heteroscedastic model we consider is

$$\mathbf{y}_i = \mathbf{x}_i + \boldsymbol{\epsilon}_i \quad \text{where} \quad \boldsymbol{\epsilon}_i \sim \mathcal{N}(\mathbf{0}, \nu_i \mathbf{I}) \quad (1)$$

assuming Gaussian noise with variance ν_i , where \mathbf{I} denotes the $D \times D$ identity matrix. In this work, we consider the case where each data sample may have its own noise variance, however, one can adapt this method to consider the case where there are G groups of data having shared noise variance terms $\{\nu_1, \dots, \nu_G\}$. Sec. III-C discusses an optimization problem based on this model that estimates the heterogeneous noise variances $\{\nu_i\}_{i=1}^N$ and the subspace basis \mathbf{U} .

B. Union of Subspaces Model ($K \geq 1$)

Let $\mathbf{Y} = [\mathbf{y}_1 \ \dots \ \mathbf{y}_N] \in \mathbb{R}^{D \times N}$ denote a matrix whose columns consist of all N data points $\mathbf{y}_i \in \mathbb{R}^D$. We generalize (1) to model the data with a union of subspaces model by

$$\begin{aligned} \mathbf{y}_i &= \mathbf{x}_i + \boldsymbol{\epsilon}_i \\ \mathbf{x}_i &= \mathbf{U}_{k_i} \mathbf{z}_i \quad \text{for some } k_i \in \{1, \dots, K\}, \end{aligned} \quad (2)$$

where $\mathbf{U}_k \in \mathbb{R}^{D \times d_k}$ is a subspace basis that has subspace dimension d_k . Here, $\mathbf{z}_i \in \mathbb{R}^{d_k}$ denotes the basis coefficients associated with \mathbf{x}_i , and $\boldsymbol{\epsilon}_i \in \mathbb{R}^D$ denotes noise for that point drawn from $\boldsymbol{\epsilon}_i \sim \mathcal{N}(\mathbf{0}, \nu_i \mathbf{I})$.

If the subspace bases were known, then one would like to find the associated subspace label $c_i \in \{1, \dots, K\}$ for each data sample by solving the following optimization problem

$$c_i = \arg \min_k \|\mathbf{y}_i - \mathbf{U}_k \mathbf{U}_k' \mathbf{y}_i\|_2^2, \quad \forall \mathbf{y}_i \in \mathbf{Y}. \quad (3)$$

This label describes the subspace association of a data point \mathbf{y}_i that has the lowest residual between the original sample and its reconstructed value given the subspace. In general, the goal is to estimate all of the subspace bases $\mathcal{U} = (\mathbf{U}_1, \dots, \mathbf{U}_K)$ and cluster assignments $\mathcal{C} = (c_1, \dots, c_N)$ associated with all the data samples.

III. RELATED WORKS

A. Subspace Clustering

Many subspace clustering algorithms fall into a general umbrella of categories such as algebraic methods [18], iterative methods [19], statistical methods [20], and spectral clustering methods [21] [22]. In recent years, both spectral clustering-based methods and iterative methods have become popular.

1) *Spectral Clustering*: Many methods build on spectral clustering. This method is often used for clustering nodes in graphs. Spectral clustering aims to find the minimum cost ‘‘cuts’’ in the graph to partition nodes into clusters. Given some collection of data points, one way to construct a graph is to assume that ‘‘nearby’’ data samples are highly connected in the graph. Thus, it is possible to construct a graph from data samples, with various levels of connectedness, by using some metric to assign affinity/similarity for each pair of points. Let $\mathcal{G}(\mathcal{V}, \mathbf{W})$ correspond to a graph that consists of vertices $\mathcal{V} = \{v_1, \dots, v_N\}$ and edge weights $\mathbf{W} \in \mathbb{R}^{N \times N}$ such that w_{ij} corresponds to some nonnegative weight, or similarity, between v_i and v_j . The graph \mathcal{G} is assumed to be undirected, i.e., $\mathbf{W} = \mathbf{W}'$. The degree of a node is defined as $d_i = \sum_{j=1}^N w_{ij}$ and can be collected to form a degree matrix such that $\mathbf{D} = \text{diag}(d_1, \dots, d_N)$. Let $\mathcal{A}_1, \dots, \mathcal{A}_K$ form a K -partition on $\mathcal{G}(\mathcal{V}, \mathbf{W})$ and $\text{cut}(\mathcal{A}, \mathcal{B}) = \sum_{i \in \mathcal{A}, j \in \mathcal{B}} w_{ij}$. Then, spectral clustering aims to solve the following

$$\arg \min_{\mathcal{A}_1, \dots, \mathcal{A}_K} \frac{1}{2} \sum_{i=1}^K \frac{\text{cut}(\mathcal{A}_i, \bar{\mathcal{A}}_i)}{|\mathcal{A}_i|} \quad (4)$$

where $\bar{\mathcal{A}}_i$ is all vertices not belonging in \mathcal{A}_i and $|\mathcal{A}_i|$ is the number of vertices belonging to the i th partition. Instead of working with \mathbf{W} directly, one computes a normalized graph Laplacian such as $\mathbf{L} = \mathbf{I} - \mathbf{D}^{-1} \mathbf{W}$ to make the influence of heavy degree nodes more similar to low degree nodes. Let $h_{i,j}$ indicate the j th cluster membership for the i th point by

$$h_{i,j} = \begin{cases} 1/\sqrt{|\mathcal{A}_j|} & \text{if } v_i \in \mathcal{A}_j \\ 0 & \text{otherwise.} \end{cases} \quad (5)$$

Collecting the indicator values into a matrix $\mathbf{H} \in \mathbb{R}^{N \times K}$, one can rewrite (4) in matrix notation as

$$\frac{1}{2} \sum_{i=1}^K \frac{\text{cut}(\mathcal{A}_i, \bar{\mathcal{A}}_i)}{|\mathcal{A}_i|} = \sum_{i=1}^K (\mathbf{H}' \mathbf{L} \mathbf{H})_{ii} = \text{Tr}(\mathbf{H}' \mathbf{L} \mathbf{H}), \quad (6)$$

where $\text{Tr}(\mathbf{H}) = \sum_i \mathbf{H}_{ii}$ denotes the trace of a matrix. The indicator vectors are discrete, which makes the problem computationally challenging. One way to relax the problem is to allow arbitrary real values for \mathbf{H} and instead solve

$$\hat{\mathbf{H}} = \arg \min_{\mathbf{H} \in \mathbb{R}^{N \times K}} \text{Tr}(\mathbf{H}' \mathbf{L} \mathbf{H}) \quad \text{s.t.} \quad \mathbf{H}' \mathbf{H} = \mathbf{I} \quad (7)$$

where the notation s.t. means subject to some conditions. Trace minimization problems with semi-unitary constraints are well-studied in the literature, and it is easy to see that $\hat{\mathbf{H}}$ consists of the first K eigenvectors of \mathbf{L} associated with the smallest eigenvalues, i.e., $\lambda_1(\mathbf{L}) \leq \dots \leq \lambda_N(\mathbf{L})$ where $\lambda_i(\mathbf{L})$ denotes the i th eigenvalue of \mathbf{L} . Once $\hat{\mathbf{H}}$ is computed, the K -means algorithm is applied to $\hat{\mathbf{H}}'$, treating each row of $\hat{\mathbf{H}}$ as the spectral embedding of the associated v_i vertex. The next section,

Sec. III-A2, now describes some subspace clustering methods that use this technique by first forming a weight matrix \mathbf{W} and then applying the spectral clustering method on \mathbf{W} .

2) *Self-Expressive Methods*: Self-expressive methods exploit the “self-expressiveness property” [23] of data that hypothesizes that a single data point can be expressed as a linear combination of other data points in its cluster, which is trivially true if the data exactly follows a subspace model. The goal is to learn those linear coefficients which is often achieved by adopting different regularizers in the formulation. These self-expressive algorithms, e.g., SSC [13] and LRSC [24], learn the coefficient matrix $\mathbf{P} \in \mathbb{R}^{N \times N}$ by solving special cases of the following general optimization problem

$$\arg \min_{\mathbf{P}} \text{DF}(\mathbf{Y} - \mathbf{Y}\mathbf{P}) + \lambda \Lambda(\mathbf{P}) \quad \text{s.t. } \mathbf{P} \in \mathcal{S}_{\mathbf{P}}. \quad (8)$$

The function $\text{DF}(\mathbf{Y} - \mathbf{Y}\mathbf{P})$ is a data fidelity term, $\Lambda(\mathbf{P})$ is a regularizer, and $\mathcal{S}_{\mathbf{P}}$ is some constrained set to encourage \mathbf{P} to satisfy certain conditions. In the case of SSC, the optimization problem is formulated as

$$\arg \min_{\mathbf{P}} \|\mathbf{Y} - \mathbf{Y}\mathbf{P}\|_{\text{F}}^2 + \lambda \|\mathbf{P}\|_{1,1} \quad \text{s.t. } \mathbf{P}_{ii} = 0 \quad \forall i \quad (9)$$

where $\|\mathbf{P}\|_{1,1} = \|\text{vec}(\mathbf{P})\|_1 = \sum_i |p_i|$ is the vectorized 1-norm and $\|\cdot\|_{\text{F}} = \|\text{vec}(\cdot)\|_2$ is the Frobenius norm of a matrix. Observe that (9) approximates each data sample as a sparse linear combination of other data points to form \mathbf{P} . Let $\text{abs}(\mathbf{P})$ represent the element-wise absolute value of matrix \mathbf{P} . Then, spectral clustering is performed on $\mathbf{W} = \frac{1}{2}(\text{abs}(\mathbf{P}') + \text{abs}(\mathbf{P}))$ by applying the K -means method to the spectral embedding of the affinity matrix \mathbf{W} . Ideally, (9) would select the high quality data to represent worse samples in \mathbf{P} and this information would be retained in \mathbf{W} . However, this data quality awareness condition is not guaranteed in self-expressive methods to our knowledge. In our experiments, Fig. 2f and Fig. 6 show that there must be an issue constructing an ideal \mathbf{P} due to worse clustering performance in heteroscedastic conditions.

3) *Subspace Clustering via Thresholding (TSC)*: In the example to follow, assume that there are two distinct 1-dimensional subspaces. Given two data samples \mathbf{y}_i and \mathbf{y}_j , intuitively their dot product $\langle \mathbf{y}_i, \mathbf{y}_j \rangle$ will be high if $c_i = c_j$, meaning they belong to the same subspace. Likewise, if $c_i \neq c_j$, then $\langle \mathbf{y}_i, \mathbf{y}_j \rangle = 0$ if the subspaces are orthogonal. In non-orthogonal scenarios, one expects $|\langle \mathbf{y}_i, \mathbf{y}_j \rangle|$ to be smaller when $c_i \neq c_j$ than when $c_i = c_j$. Using this idea, in more general D -dimensional subspace settings, TSC constructs a matrix $\mathbf{Z} \in \mathbb{R}^{N \times N}$ that describes similarity such that

$$\mathbf{Z}_{ij} = \exp(-2 \arccos(|\langle \mathbf{y}_i, \mathbf{y}_j \rangle|)) \quad \text{s.t. } \mathbf{Z}_{ii} = 0 \quad \forall i. \quad (10)$$

This matrix is then thresholded to retain only the top q values for each row, i.e.,

$$\mathbf{W} = \arg \min_{\mathbf{W}} \|\mathbf{W} - \mathbf{Z}\|_{\text{F}}^2 \quad \text{s.t. } \|\mathbf{W}_{i,:}\|_0 = q \quad \forall i \quad (11)$$

where $\|\mathbf{W}_{i,:}\|_0 = q$ is the l_0 pseudo-norm that counts the number of nonzero entries. In other words, one constructs $\mathbf{W}_{i,:}$ using the q nearest neighbors that correspond to the highest magnitude values. Then, spectral clustering is applied to \mathbf{W} to find the cluster associations.

4) *Ensemble K -Subspaces (EKSS)*: Iterative methods are based on the idea of alternating between cluster assignments and subspace basis approximation, with KSS being highly prominent [25]. The KSS algorithm seeks to solve

$$\arg \min_{\mathcal{C}, \mathcal{U}} \sum_{k=1}^K \sum_{c_i=k, \forall i} \|\mathbf{y}_i - \mathbf{U}_k \mathbf{U}_k' \mathbf{y}_i\|_2^2. \quad (12)$$

The goal is to minimize the sum of residual norms by alternating between performing PCA on each cluster to update \mathcal{U} and using the subspace bases to calculate new cluster assignments \mathcal{C} in a similar fashion to the K -means algorithm. The quality of the solution depends highly on the initialization. Recent work provides convergence guarantees and spectral initialization schemes that provably perform better than random initialization [26]. However, this problem (12), is known to be NP-hard [27]. Further, it is prone to local minima [28]. To overcome this, consensus clustering [29] is a tool that leverages information from many trials and combines results together. This approach, known as Ensemble KSS (EKSS) [16], creates an affinity matrix whose (i, j) th entry represents the number of times the two points were clustered together in a trial. Then, spectral clustering is performed on the affinity matrix to get the final clustering from the many base clusterings. The use of PCA makes it challenging to learn clusters and subspace bases in the heteroscedastic regime since PCA implicitly assumes the same noise variance across all samples [30]. The proposed ALPCAHUS approach in Sec. IV builds on KSS, and its ensemble version, by generalizing (12) to the heteroscedastic regime while simultaneously learning data quality.

B. Other heteroscedastic models

This paper focuses on heteroscedastic noise across the data samples. There are other *subspace learning* methods in the literature that explore heteroscedasticity in different ways. For example, HeteroPCA considers heteroscedasticity across the feature space [31]. One possible application of that model is for data that consists of sensor information with multiple devices that naturally have different levels of precision and signal to noise ratio. Another heterogeneity model considers the noise to be homoscedastic and instead assumes that the signal itself is heteroscedastic [32]. That work considers applications where the power fluctuating signals, i.e., heteroscedastic signals, are embedded in white Gaussian noise. However, to the authors' knowledge, there are no algorithms for *subspace clustering* that consider feature-space heteroscedasticity. We exclude comparisons with these methods since their models are very different and each have their own applications.

C. Single Subspace Heteroscedastic PCA

Before extending (12) to the heteroscedastic setting, we will review how LR-ALPCAH [17] solves for a single subspace ($K = 1$) in the heteroscedastic setting using the model described in (1). For the measurement model $\mathbf{y}_i \sim \mathcal{N}(\mathbf{x}_i, \nu_i \mathbf{I})$ in (1), the probability density function for a single data sample \mathbf{y}_i following a Gaussian distribution is easily expressed as

$$\frac{1}{\sqrt{(2\pi)^D |\nu_i \mathbf{I}|}} \exp \left[-\frac{1}{2} (\mathbf{y}_i - \mathbf{x}_i)' (\nu_i \mathbf{I})^{-1} (\mathbf{y}_i - \mathbf{x}_i) \right]. \quad (13)$$

For independent samples, after dropping constants, the joint log likelihood of all data $\{\mathbf{y}_i\}_{i=1}^N$ is the following

$$\sum_{i=1}^N -\frac{1}{2} \log |\nu_i \mathbf{I}| - \frac{1}{2} (\mathbf{y}_i - \mathbf{x}_i)' (\nu_i \mathbf{I})^{-1} (\mathbf{y}_i - \mathbf{x}_i). \quad (14)$$

Let $\mathbf{\Pi} = \text{diag}(\nu_1, \dots, \nu_N) \in \mathbb{R}^{N \times N}$ be a diagonal matrix representing the typically unknown noise variances. Then, the negative log likelihood in matrix form is

$$\frac{D}{2} \log |\mathbf{\Pi}| + \frac{1}{2} \text{Tr}[(\mathbf{Y} - \mathbf{X})\mathbf{\Pi}^{-1}(\mathbf{Y} - \mathbf{X})']. \quad (15)$$

After further manipulation by trace lemmas, we rewrite the negative log-likelihood as

$$\frac{1}{2} \|(\mathbf{Y} - \mathbf{X})\mathbf{\Pi}^{-1/2}\|_{\text{F}}^2 + \frac{D}{2} \log |\mathbf{\Pi}|. \quad (16)$$

Our previous work used a functional operator similar to the nuclear norm to regularize \mathbf{X} and encourage a low-rank solution by penalizing the tail sum of singular values [33] [34]. However, this method named ALPCAH was relatively slow due to SVD operations every iteration. To reduce computation and enforce a low-rank solution, the LR-ALPCAH variant [17] took inspiration from the matrix factorization literature [35] and factorized $\mathbf{X} \in \mathbb{R}^{D \times N} \approx \mathbf{L}\mathbf{R}'$ where $\mathbf{L} \in \mathbb{R}^{D \times \hat{d}}$ and $\mathbf{R} \in \mathbb{R}^{N \times \hat{d}}$ for some rank estimate \hat{d} . Using this idea, LR-ALPCAH estimates \mathbf{X} by solving for \mathbf{L} and \mathbf{R} , jointly with noise variance matrix $\mathbf{\Pi}$, by the following

$$\arg \min_{\mathbf{L}, \mathbf{R}, \mathbf{\Pi}} \frac{1}{2} \|(\mathbf{Y} - \mathbf{L}\mathbf{R}')\mathbf{\Pi}^{-1/2}\|_{\text{F}}^2 + \frac{D}{2} \log |\mathbf{\Pi}|. \quad (17)$$

This comes from a modified model of (1) described by

$$\mathbf{y}_i = \mathbf{L}\mathbf{r}_i + \boldsymbol{\epsilon}_i, \quad \boldsymbol{\epsilon}_i \sim \mathcal{N}(\mathbf{0}, \nu_i \mathbf{I}) \quad (18)$$

where \mathbf{r}_i denotes the i th column of \mathbf{R} . Sec. IV combines ideas from (12) and (17) to tackle the union of subspaces setting.

IV. PROPOSED SUBSPACE CLUSTERING METHOD

For notational simplicity, let $\mathbf{Y}_k = \mathbf{Y}_{\mathcal{C}_k} \in \mathbb{R}^{D \times N_k}$ denote the submatrix of \mathbf{Y} having columns corresponding to data samples that are estimated to belong in the k th subspace, i.e., $\mathbf{Y}_k = \mathbf{Y}_{\mathcal{C}_k} = \text{matrix}(\{\mathbf{y}_i : c_i = k\})$, where $\mathcal{C}_k = \{i : c_i = k\}$ must be determined. This notation applies similarly to other matrices such as $\mathbf{\Pi}_k = \mathbf{\Pi}_{\mathcal{C}_k} = \text{diag}(\{\nu_i : c_i = k\})$. For the union of subspace measurement model in (2), we generalize LR-ALPCAH (17) by proposing the following cost function

$$\arg \min_{\mathcal{L}, \mathcal{R}, \mathbf{\Pi}, \mathcal{C}} \underbrace{\sum_{k=1}^K \frac{1}{2} \left\| (\mathbf{Y}_k - \mathbf{L}_k \mathbf{R}_k') \mathbf{\Pi}_k^{-1/2} \right\|_{\text{F}}^2 + \frac{D}{2} \log |\mathbf{\Pi}_k|}_{f(\mathcal{L}, \mathcal{R}, \mathbf{\Pi}, \mathcal{C})} \quad (19)$$

where \mathcal{C} , $\mathbf{\Pi}$, \mathcal{L} , \mathcal{R} denote the sets of estimated clusters, noise variances, and factorized matrices respectively for each cluster $k = 1, \dots, K$. Specifically, $\mathcal{L} \triangleq \{\mathbf{L}_1, \dots, \mathbf{L}_K\}$ and $\mathcal{R} \triangleq \{\mathbf{R}_1, \dots, \mathbf{R}_K\}$. Our algorithm for solving (19) is called ALPCAHUS (ALPCAH for Union of Subspaces). We solve (19) via alternating minimization, and the method alternates

between subspace basis estimation and data sample reassignment/clustering. We begin with subspace basis estimation.

Firstly, with data sample assignments fixed, $\forall k \in \{1, \dots, K\}$ we estimate subspace bases by applying T_1 iterations of alternating minimization by

$$\begin{aligned} (\mathbf{L}_k^{(T_1)}, \mathbf{R}_k^{(T_1)}, \mathbf{\Pi}_k^{(T_1)}) &= \arg \min_{\mathbf{L}_k, \mathbf{R}_k, \mathbf{\Pi}_k} f_k(\mathbf{L}_k, \mathbf{R}_k, \mathbf{\Pi}_k; \mathbf{Y}_k) \\ &\text{s.t. } \mathbf{\Pi}_k \succeq \alpha \mathbf{I}. \end{aligned} \quad (20)$$

The solution to (20) is described in Ref. [17]. However, for completeness and notational consistency, the updates are included in (21), (22), and (24). Given the current t_1 iteration, the updates for the $t_1 + 1$ iteration are given as

$$\begin{aligned} \mathbf{L}_k^{(t_1+1)} &= \arg \min_{\mathbf{L}_k} f_k(\mathbf{L}_k, \mathbf{R}_k^{(t_1)}, \mathbf{\Pi}_k^{(t_1)}; \mathbf{Y}_k^{(t_2)}) \\ &= \mathbf{Y}_k^{(t_2)} \mathbf{\Pi}_k^{(t_1)} \mathbf{R}_k^{(t_1)} \left((\mathbf{R}_k^{(t_1)})' \mathbf{\Pi}_k^{(t_1)} \mathbf{R}_k^{(t_1)} \right)^{-1} \end{aligned} \quad (21)$$

$$\begin{aligned} \mathbf{R}_k^{(t_1+1)} &= \arg \min_{\mathbf{R}_k} f_k(\mathbf{L}_k^{(t_1+1)}, \mathbf{R}_k, \mathbf{\Pi}_k^{(t_1)}; \mathbf{Y}_k^{(t_2)}) \\ &= (\mathbf{Y}_k^{(t_2)})' \mathbf{L}_k^{(t_1+1)} \left((\mathbf{L}_k^{(t_1+1)})' \mathbf{L}_k^{(t_1+1)} \right)^{-1}. \end{aligned} \quad (22)$$

Further, estimate the noise variance terms by

$$\max \left(\alpha, \frac{1}{|D|} \underbrace{\left\| (\mathbf{Y}_k^{(t_2)} - \mathbf{L}_k^{(t_1+1)} (\mathbf{R}_k^{(t_1+1)})') e_i \right\|_2^2}_{p_k(i)} \right) \quad (23)$$

where e_i denotes the i th canonical basis vector that is used to select the i th residual column and $\alpha > 0$ is a user-selected noise variance threshold parameter. Then, we update the noise variance matrix $\mathbf{\Pi}_k$ as follows

$$\begin{aligned} \mathbf{\Pi}_k^{(t_1+1)} &= \arg \min_{\mathbf{\Pi}_k} f_k(\mathbf{L}_k^{(t_1+1)}, \mathbf{R}_k^{(t_1+1)}, \mathbf{\Pi}_k; \mathbf{Y}_k^{(t_2)}) \\ &= \text{diag}(p_k(1), \dots, p_k(|\mathcal{C}_k|)). \end{aligned} \quad (24)$$

Because $\mathbf{\Pi}_k$ is a diagonal matrix, the $\mathbf{\Pi}_k \succeq \alpha \mathbf{I}$ majorization condition in (20) being equivalent to $\forall i, \lambda_i(\mathbf{\Pi}_k) \geq \alpha$ implies that $\forall i, \nu_i > \alpha$. This leads to a projection to the positive set $[\alpha, \infty)$ by the $\max(\alpha, \cdot)$ condition in (23). This condition is sufficient to ensure convergence as proven in [17, Thm. 2] and used in this work to further prove ALPCAHUS convergence in Thm. 1 using some $\alpha \in \mathbb{R}_+$.

Secondly, fixing the subspaces, we update the data sample assignments to clusters. The cluster update is essentially $\mathcal{C}^{\text{new}} = \arg \min_{\mathcal{C}} f(\mathcal{L}, \mathcal{R}, \mathbf{\Pi}, \mathcal{C})$, with a rule to break ties in favor of the previous cluster assignment as follows. Let $\mathbf{U}_k^{(T_1)}$ denote the Gram-Schmidt vectors of $\mathbf{L}_k^{(T_1)}$. Define residual point error for k th basis by

$$J_i(k) = \left\| \mathbf{y}_i - \mathbf{U}_k^{(T_1)} \left(\mathbf{U}_k^{(T_1)} \right)' \mathbf{y}_i \right\|_2^2 \quad (25)$$

and let the set \mathcal{S}_{J_i} denote the set of minimizers of $J_i(k)$ by

$$\mathcal{S}_{J_i} = \arg \min_k J_i(k). \quad (26)$$

Then $\forall i$, given the label estimate $c_i^{(t_2)}$ for the t_2 iteration, compute the next label by

$$c_i^{(t_2+1)} = \begin{cases} c_i^{(t_2)} & \text{if } c_i^{(t_2)} \in \mathcal{S}_{J_i} \\ k^* \in \mathcal{S}_{J_i} & \text{otherwise.} \end{cases} \quad (27)$$

Algorithm ALPCHUS (unknown noise variances, unknown noise grouping, ensemble version with random init.)

```

1: Input:  $\mathbf{Y} \in \mathbb{R}^{D \times N}$ : data,  $K \in \mathbb{Z}^+$ : number of subspaces,  $\{\hat{d}_k \in \mathbb{Z}^+ \ \forall k \in \{1, \dots, K\}\}$ : candidate dimension for all
   clusters,  $q \in \mathbb{Z}^+$ : threshold parameter,  $B \in \mathbb{Z}^+$ : base clusterings,  $T_1 \in \mathbb{Z}^+$ : LR-ALPCHUS iterations,  $T_2 \in \mathbb{Z}^+$ : maximum
   alternating updates (cluster reassignments)
2: Output:  $\mathcal{C}_S = \{c_1, \dots, c_N\}$ : clusters of  $\mathbf{Y}$ 
3: for  $b = 1, \dots, B$  (in parallel) do
4:    $\mathcal{C}_k \sim \{1, \dots, N\}$  s.t.  $|\mathcal{C}_k| \approx \frac{N}{K}$  for  $k = 1, \dots, K$  Initialize clusters randomly
5:    $\mathbf{\Pi}_k \leftarrow \mathbf{I}$  for  $k = 1, \dots, K$  Assume homoscedastic data initially
6:    $\mathbf{L}_k, \mathbf{R}_k \leftarrow \mathbf{U}_{:,1:\hat{d}_k} \mathbf{\Sigma}_{1:\hat{d}_k,1:\hat{d}_k}^{1/2}, \mathbf{\Sigma}_{1:\hat{d}_k,1:\hat{d}_k}^{1/2} \mathbf{V}_{:,1:\hat{d}_k}$  where  $\text{SVD}(\mathbf{Y}_{\mathcal{C}_k}) = \mathbf{U}\mathbf{\Sigma}\mathbf{V}'$  for  $k = 1, \dots, K$  Spectral init
7:   for  $t_2 = 1, \dots, T_2$  (in sequence) do
8:      $\mathbf{L}_k, \mathbf{R}_k, \mathbf{\Pi}_k \leftarrow$  Compute (21)-(24) using  $\mathbf{Y}_{\mathcal{C}_k}$  for  $T_1$  iterations for  $k = 1, \dots, K$  Apply LR-ALPCHUS [17]
9:      $\mathcal{C}_k \leftarrow \{\forall \mathbf{y}_i \in \mathbf{Y} : \forall k, \text{ apply (25)-(27) with } \mathbf{U}_k \text{ extracted from GramSchmidt}(\mathbf{L}_k)\}$  Update cluster labels
10:    Stop execution if  $\mathcal{C}_k^{(t_2+1)} = \mathcal{C}_k^{(t_2)}$  is met for all clusters Stopping criteria
11:   end for
12:    $\mathcal{C}^{(b)} \leftarrow \mathcal{C} = \{c_1, \dots, c_N\}$  Collect results from all trials
13: end for
14:  $\mathbf{A}_{i,j} \leftarrow$  Form  $\mathbf{A}$  by (28) using  $\{\mathcal{C}^{(1)}, \dots, \mathcal{C}^{(B)}\}$  Form affinity matrix of similar clusterings
15:  $\mathbf{Z}^{\text{row}} \leftarrow$  Threshold rows by solving (29) using  $\mathbf{A}$  Retain top  $q$  elements for each row
16:  $\mathbf{Z}^{\text{col}} \leftarrow$  Threshold columns by solving (30) using  $\mathbf{A}$  Retain top  $q$  elements for each column
17:  $\mathbf{W} \leftarrow \frac{1}{2}(\mathbf{Z}^{\text{row}} + \mathbf{Z}^{\text{col}})$  Average affinity matrix
18:  $\mathcal{C}_S \leftarrow$  Perform spectral clustering on  $\mathbf{W}$  via (4)-(7) Final clustering

```

The solution to (27) involves the following procedure. Given a data sample \mathbf{y}_i , find the lowest subspace projection residual of all subspaces by (25) and assign it to $c_i^{(t_2+1)}$ at the $t_2 + 1$ iteration. In the event of a tie, meaning there is more than one subspace that has equal residual, retain the past label $c_i^{(t_2)}$ for the new label $c_i^{(t_2+1)}$. By doing this, cycling between labels is prevented for all data samples. This cluster reassignment criteria will be important to ensure convergence as proven in Thm. 1. Because (26) is with respect to k and not the i th sample, a residual weighted with the noise parameter ν_i is unnecessary, since it would not change the minimizing k .

To further improve clustering performance, consensus clustering can be leveraged over many trials. Initially, we tried using this approach with only one trial as seen in Fig. 2b and ALPCHUS ($B = 1$) result in Fig. 6a. However, since K -subspaces in general is sensitive to initialization, during experimentation we found higher clustering accuracy by using a consensus approach with more than one trial as shown in Fig. 2d and ALPCHUS ($B = 16$) result in Fig. 6a.

A. Ensemble Extension for ALPCHUS

This section presents the ensemble algorithm with base clustering parameter B to combine multiple trials for finding \mathcal{C} in (19). ALPCHUS with $B > 1$ leverages consensus clustering by forming an affinity matrix $\mathbf{A} \in \mathbb{R}^{N \times N}$ where

$$\mathbf{A}_{i,j} = \frac{1}{B} |\{\forall b \in \{1, \dots, B\} \text{ such that } \mathbf{y}_i, \mathbf{y}_j \text{ are co-clustered in } \mathcal{C}^{(b)}\}| \quad (28)$$

and $\mathcal{C}^{(b)} = \{c_1^{(b)}, \dots, c_N^{(b)}\}$ refers to the cluster labels for the b th trial ranging from 1 to B . Then, the rows and columns of \mathbf{W} are thresholded to retain the top q values by solving

$$\mathbf{Z}^{\text{row}} = \arg \min_{\mathbf{Z}} \|\mathbf{A} - \mathbf{Z}\|_{\text{F}}^2 \quad \text{s.t.} \quad \|\mathbf{Z}_{i,:}\|_0 = q \quad \forall i \quad (29)$$

$$\mathbf{Z}^{\text{col}} = \arg \min_{\mathbf{Z}} \|\mathbf{A} - \mathbf{Z}\|_{\text{F}}^2 \quad \text{s.t.} \quad \|\mathbf{Z}_{:,i}\|_0 = q \quad \forall i. \quad (30)$$

Finally, spectral clustering is applied to $\mathbf{W} = \frac{1}{2}(\mathbf{Z}^{\text{col}} + \mathbf{Z}^{\text{row}})$ to get the clusters from the results of the ensemble. This spectral clustering operation assumes a balanced cluster distribution that may not hold in practice. All of our included experiments contain balanced cluster sizes; however, Sec. VIII-B provides discussion of this limitation and possible remediation strategies.

The q threshold parameter can be set by cross validation, which is what is done in the experiments shown in Sec. V, or other techniques can be used. For example, Ref. [36] creates a sparse L2 graph through hard thresholding to retain the top $q = d_k$ values where d_k is the known subspace dimension. Thus, q can be tied to the true or estimated subspace dimension instead. Sec. VIII-C provides more discussion on ALPCHUS hyperparameters including recommended values.

In this more general ensemble framework, one could select $B = 1$ to reduce to one trial of the optimization problem in (19) which is the non-ensemble version of ALPCHUS. Alg. ALPCHUS summarizes the procedure for subspace clustering with optional ensemble learning. For Julia code implementations, refer to <https://github.com/javersc1/ALPCHUS>.

B. ALPCHUS Convergence

In the single cluster setting, ALPCHUS with $K = 1$ has a sequence of cost function values $f_1(\mathbf{L}_1, \mathbf{R}_1, \mathbf{\Pi}_1; \mathbf{Y}_1)$ that provably converges to local minima, since the cost function and algorithm simplify to LR-ALPCHUS (17) that has convergence guarantees as proven in Ref. [17, Thm. 2]. In the multi-cluster setting with $K > 1$, Thm. 1 below shows that the sequence of cost function values produced by $f(\mathcal{L}, \mathcal{R}, \mathbf{\Pi}, \mathcal{C})$ in (19) converges asymptotically. The argument in Thm. 1 below is a natural extension of that in the original k -subspaces paper

[25, Thm. 7] with greater mathematical exposé. Sec. VIII-A provides an experimental result that corroborates this theorem.

Theorem 1. Consider the ALPCAHUS cost function $f(\mathcal{L}, \mathcal{R}, \mathbf{\Pi}, \mathcal{C})$ in (19). Assume a noise variance threshold parameter $\alpha \in \mathbb{R} > 0$ that lower bounds all ν_i , and the cluster assignment criteria in (27) that accepts changes only if there is a cluster reassignment of points that strictly decreases the cost function $f(\cdot)$, as expressed in (27). Then, (19) generates a sequence of cost function values that converges asymptotically. Furthermore, the algorithm terminates in finite iterations due to stopping criteria in line (10) of Alg. ALPCAHUS that checks whether clusters have changed from the previous iteration.

Proof. To prove that the sequence of cost function values converges, we show that each step decreases the cost function. We also show that the algorithm terminates at a point where the variables stop changing. Each step consists of two sub-steps: first, the subspace estimation sub-step where LR-ALPCAH is used, and second, the clustering sub-step where projection onto the estimated subspaces is done. Let t_1 be the iteration variable associated with the variables in the subspace estimation sub-step and t_2 be the iteration variable associated with the variables in the clustering sub-step. Define $\mathbf{X}_k = \mathbf{L}_k \mathbf{R}'_k$ and bound the cost by

$$\begin{aligned} f(\mathcal{L}^{(t_1)}, \mathcal{R}^{(t_1)}, \mathbf{\Pi}^{(t_1)}, \mathcal{C}^{(t_2)}) &= \\ \frac{1}{2} \sum_k \sum_{i \in \mathcal{C}_k^{(t_2)}} \frac{1}{\nu_i^{(t_1)}} \left\| [\mathbf{Y}_k]_i - [\mathbf{X}_k]_i^{(t_1)} \right\|_2^2 + D \log \nu_i^{(t_1)} & \quad (31) \\ \geq \frac{1}{2} \sum_k \sum_{i \in \mathcal{C}_k^{(t_2)}} \frac{1}{\nu_i^{(t_1+1)}} \left\| [\mathbf{Y}_k]_i - [\mathbf{X}_k]_i^{(t_1+1)} \right\|_2^2 & \\ + D \log \nu_i^{(t_1+1)} = f(\mathcal{L}^{(t_1+1)}, \mathcal{R}^{(t_1+1)}, \mathbf{\Pi}^{(t_1+1)}, \mathcal{C}^{(t_2)}) & \quad (32) \\ \geq \frac{1}{2} \sum_k \sum_{i \in \mathcal{C}_k^{(t_2+1)}} \frac{1}{\nu_i^{(t_1+1)}} \left\| [\mathbf{Y}_k]_i - [\mathbf{X}_k]_i^{(t_1+1)} \right\|_2^2 & \\ + D \log \nu_i^{(t_1+1)} = f(\mathcal{L}^{(t_1+1)}, \mathcal{R}^{(t_1+1)}, \mathbf{\Pi}^{(t_1+1)}, \mathcal{C}^{(t_2+1)}) & \quad (33) \end{aligned}$$

Here, (31) \geq (32) is due to the subspace step not increasing the cost for each f_k term as shown in Ref. [17, Thm. 2], and (32) \geq (33) is due to the cluster reassignment criteria in (27) only updating the cluster label that decreases (25). What has been shown is that

$$f^{(t_1, t_2)} \geq f^{(t_1+1, t_2)} \geq f^{(t_1+1, t_2+1)} \quad (34)$$

where $f^{(t_1, t_2)} = f(\mathcal{L}^{(t_1)}, \mathcal{R}^{(t_1)}, \mathbf{\Pi}^{(t_1)}, \mathcal{C}^{(t_2)})$. Thus, as the cluster assignments and subspace bases are updated, the cost is non-increasing. Since the cost function values are non-increasing at every step, bounded below, then the sequence of cost function values produced by (19) converges asymptotically. Furthermore, the stopping criteria in line (10) ensures that the algorithm terminates when all clusters do not change. Because there are only a finite number of ways to assign cluster labels, Alg. ALPCAHUS will stop after a finite number of iterations. \square

C. Rank Estimation

In subspace clustering, some algorithms like SSC do not require subspace dimension to be known or estimated, whereas others like KSS require it. For the group of algorithms that require this parameter, there is great interest in adaptive methods that can learn the subspace dimension. In recent work, Ref. [26] proposed using an eigengap heuristic on the sample covariance matrix of each cluster to estimate dimension. Mathematically, this means calculating the following

$$\mathbf{S}_k = \frac{1}{|\mathcal{C}_k|} \mathbf{Y}_k \mathbf{Y}'_k \quad (35)$$

$$\hat{d}_k = \arg \max_i |\lambda_i(\mathbf{S}_k) - \lambda_{i+1}(\mathbf{S}_k)| \quad (36)$$

where $\lambda_i(\mathbf{S}_k)$ denotes the i th eigenvalue of \mathbf{S}_k assuming $\lambda_1 \geq \dots \geq \lambda_D$. For heteroscedastic data, the eigengap heuristic can break down, making it challenging to determine rank, as shown in Sec. V, Fig. 5. In recent work, Ref. [37] developed a parallel analysis algorithm to estimate the rank of a matrix that is consistently shown to work well in the heteroscedastic regime if the data comes from a *single* subspace only. It works by creating an i.i.d. Bernoulli ($p = 0.5$) matrix denoted as \mathbf{M} and analyzing the singular values of $\mathbf{M} \odot \mathbf{Y}$ for a matrix of data samples \mathbf{Y} . One can distinguish what singular values are associated with the signal and noise component of the data through this process. We generalize this line of work and apply it to the union of subspace setting by starting off over-parameterized and adaptively shrinking the bases by

$$\begin{aligned} \forall k \in \{1, \dots, K\} \text{ do} & \\ \tilde{\sigma}^{(r)} = \text{SingularValues}(\mathbf{M} \odot \mathbf{Y}_k) \quad \forall r \in \{1, \dots, R\} & \quad (37) \\ \hat{d}_k = \text{smallest } d \text{ that satisfies} & \\ \sigma_{d+1}(\mathbf{Y}_k) \leq \alpha\text{-percentile of } \{\tilde{\sigma}_{d+1}^{(1)}, \dots, \tilde{\sigma}_{d+1}^{(R)}\}. & \quad (38) \end{aligned}$$

This is done for each estimated cluster \mathbf{Y}_k over R random trials where $1 \leq R \ll T_2$, and T_2 denotes the maximum ALPCAHUS iterations. Here, $\sigma_{d+1}(\mathbf{Y}_k)$ denotes the $d+1$ singular value of \mathbf{Y}_k . This process is repeated for all cluster subsets $\{\mathbf{Y}_1, \dots, \mathbf{Y}_K\}$ after the cluster reassignment update in (27). To reduce computation, this dimension estimation is performed sparingly in the ALPCAHUS method.

D. Cluster Initialization

For the non-ensemble version of ALPCAHUS ($B = 1$), it previously remained to be seen whether there exists an initialization scheme that performs better than random cluster assignment in the heteroscedastic regime. In recent work, Ref. [26] proposed a thresholding inner-product based spectral initialization method (TIPS), designed for homoscedastic data to be used with KSS, where an affinity matrix is generated by $\mathbf{W}_{ij} = 1$ if $|\langle \mathbf{y}_i, \mathbf{y}_j \rangle| \geq \tau$ and $i \neq j$ given a thresholding parameter $\tau > 0$. Instead, in this work, we generate a fully connected \mathbf{W} by creating

$$\mathbf{W}_{ij} = |\langle \mathbf{y}_i, \mathbf{y}_j \rangle| \text{ if } i \neq j, 0 \text{ otherwise,} \quad (39)$$

and hard threshold to retain the top q edges by solving (11) so that $\tau = q$ for simplicity. Then, the cluster assignments $\mathcal{C} =$

$\{c_1, \dots, c_N\}$ are calculated by applying the spectral clustering method on the thresholded \mathbf{W} . Recall that $\mathbf{y}_i = \mathbf{x}_i + \boldsymbol{\epsilon}_i$. Upon closer analysis, this metric in expectation, ignoring absolute value, gives

$$\begin{aligned} \mathbb{E}[\langle \mathbf{y}_i, \mathbf{y}_j \rangle] &= \mathbb{E}[\langle \mathbf{x}_i, \mathbf{x}_j \rangle] + \mathbb{E}[\langle \mathbf{x}_i, \boldsymbol{\epsilon}_j \rangle] \\ &\quad + \mathbb{E}[\langle \boldsymbol{\epsilon}_i, \mathbf{x}_j \rangle] + \mathbb{E}[\langle \boldsymbol{\epsilon}_i, \boldsymbol{\epsilon}_j \rangle] = \mathbb{E}[\langle \mathbf{x}_i, \mathbf{x}_j \rangle]. \end{aligned} \quad (40)$$

Therefore, the metric is independent of the noise variances, meaning the affinity matrix constructed does not have highly unbalanced, asymmetric edge weights from noisy samples. Thus this metric is more robust to heteroscedastic noise than others such as Euclidean norm where

$$\mathbb{E}[\|\mathbf{y}_i - \mathbf{y}_j\|_2^2] = \|\mathbf{x}_i - \mathbf{x}_j\|_2^2 + D(\nu_i + \nu_j). \quad (41)$$

Clearly, this is inflated by the noise terms ν_i and ν_j . To note, TIPS initialization is only useful when $B = 1$ for one base clustering since it is a deterministic initialization; it provably performs better than random initialization as illustrated in Fig. 4. Otherwise, random initialization is used when $B > 1$ to leverage consensus information in the ensemble process.

V. EXPERIMENTS

A. Synthetic Experiments

1) *Experimental Setup*: A synthetic dataset is generated consisting of $K = 2$ clusters each of dimension $d = 3$ derived from random subspaces in $D = 100$ dimensional ambient space. Each cluster consisted of two data groups with group 1 containing $N_1 = 6$ samples, to explore the data constrained regime, with noise variance $\nu_1 = 0.1$ per cluster. For group 2, the N_2 samples and noise variance ν_2 are varied. Cross validation is done for hyperparameters in any algorithms that require it with a separate training set. For a more detailed description of ALPCAUS parameters, including recommended default values, see Sec. VIII-C. Both the estimated clusters from each clustering algorithm and the known clusters are necessary to calculate clustering error. Further, the problem of label permutations is dealt with by using the Hungarian algorithm [38]. More concretely, clustering error (%) is defined as

$$\text{clustering error} = \frac{100}{N} \left(1 - \max_{\pi} \sum_{i,j} Q_{\pi(ij)}^{\text{out}} Q_{ij}^{\text{true}} \right) \quad (42)$$

where π is a permutation of cluster labels found by applying the Hungarian algorithm, and \mathbf{Q}^{out} and \mathbf{Q}^{true} are output labels and ground truth labelings of the data where the (i, j) th entry is one if point j belongs to cluster i and zero otherwise.

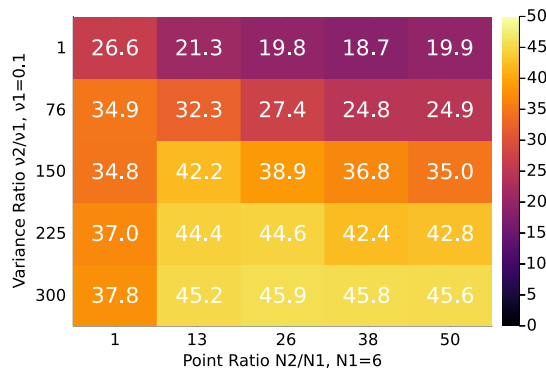
The average clustering error is computed out of 100 trials where each trial had different noise, basis coefficients, and subspace basis realizations for the clusters. Various subspace clustering algorithms are included such as K -Subspaces (KSS) [14], Ensemble K -Subspaces (EKSS) [16], Subspace Clustering via Thresholding (TSC) [39], and Doubly Stochastic Sparse Subspace Clustering (ADSSC) [40] which is a modern variant of SSC. Applying general non-subspace clustering methods such as K -means [41] resulted in poor clustering error so results of these methods are not shown in general.

2) *Clustering Error*: Table 2h shows the clustering quality of these algorithms for synthetic heteroscedastic data. Fig. 2 complements Table 2h by exploring the complete heteroscedastic landscape with a visual representation that is easier to understand. We define a method called ‘‘noisy oracle’’ where an oracle uses the true cluster assignments to apply PCA only on the low noise data for each cluster. Using these subspace basis estimates of each cluster, the oracle performs cluster assignments using (27). This oracle reference provides a kind of lower bound on realistic clustering performance since it can approximate subspace bases separately given the true labeling.

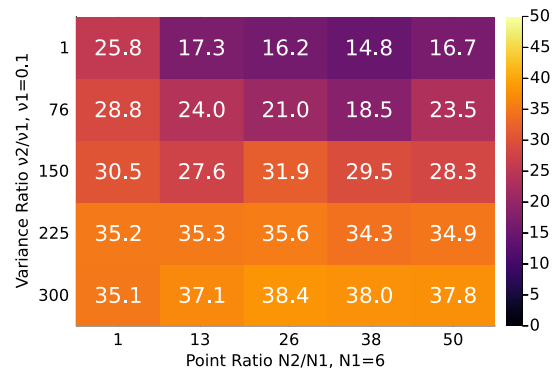
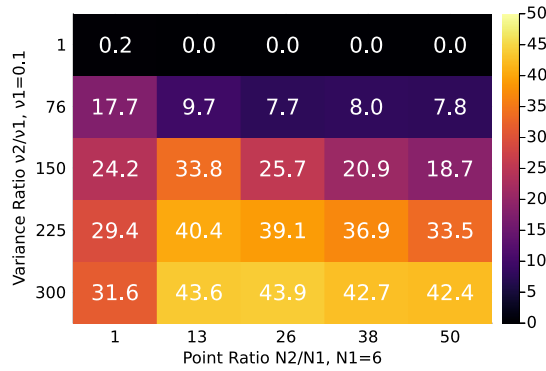
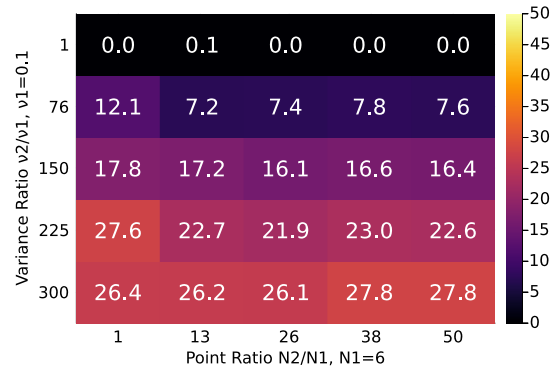
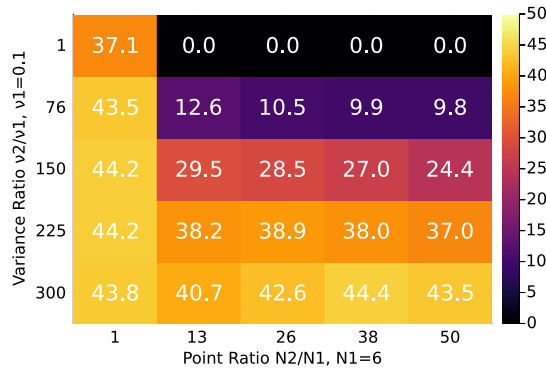
ALPCAUS ($B = 1$) with TIPS initialization achieved lower clustering error than KSS with TIPS initialization. For the ensemble methods ($B > 1$), both EKSS and ALPCAUS significantly improved. However, EKSS still had higher clustering error in more heteroscedastic regions. Meanwhile, ALPCAUS remained very close to the noisy oracle, indicating it more accurately estimated the underlying true labeling. Compared to other methods like TSC and ADSSC, ALPCAUS generally outperformed them. Overall, the ensemble version of ALPCAUS was generally more robust against heteroscedasticity compared to other subspace clustering algorithms. To summarize, the effects of data quality and data quantity is explored on the heteroscedastic landscape. To our knowledge, this is the first systematic analysis of heteroscedasticity effects on subspace clustering quality in the literature.

3) *Effects of Good Data*: Additionally, the effects of good data quantity on the subspace clustering problem is explored to understand at what point it becomes advantageous to use ALPCAUS over KSS methods. The following parameters are fixed $\{\nu_1 = 0.1, N_2 = 500\}$ and the following vary $\{N_1, \nu_2\}$. The reporting metric is the percentage difference of EKSS clustering error (%) - ALPCAUS clustering error (%), i.e., $\text{error}_{\text{EKSS}} - \text{error}_{\text{ALPCAUS}}$, meaning higher values indicate that ALPCAUS is better than EKSS. Fig. 3 shows that ALPCAUS performed better than EKSS even up to $N_1 = 160$ which represents about 33% of the total data. ALPCAUS never performed worse than EKSS but the advantage gap narrowed as N_1 increased. Thus, there is a wide range of conditions for which ALPCAUS is preferable to homoscedastic methods.

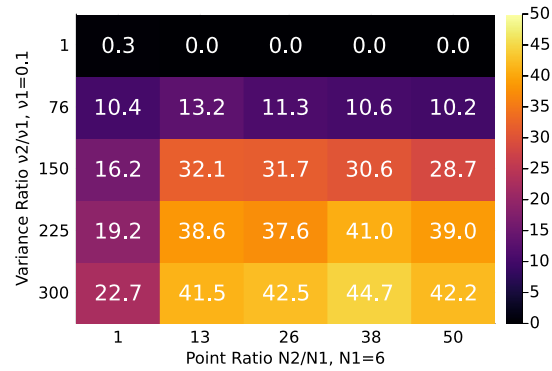
4) *Clustering Initialization*: Sec. IV-D proposed using the TIPS initialization scheme in the heteroscedastic context since the dot product metric used to construct the affinity matrix in (40) is provably robust to heteroscedastic noise. We fixed the following parameters $\{N_1, N_2\}$ and varied ν_2 while keeping $\nu_1 = 0.1$. The noisy oracle result is included to establish a realistic performance baseline. Fig. 4 shows that TIPS initialization ALPCAUS ($B = 1$) outperformed random initialization for the non-ensemble ALPCAUS method ($B = 1$) across the entire heteroscedastic landscape. Thus, TIPS should always be used for the non-ensemble version for higher clustering accuracy. The ensemble version of ALPCAUS ($B > 1$) is not included in these results because the ensemble process inherently takes advantage of random initialization to achieve a different labeling for each trial.



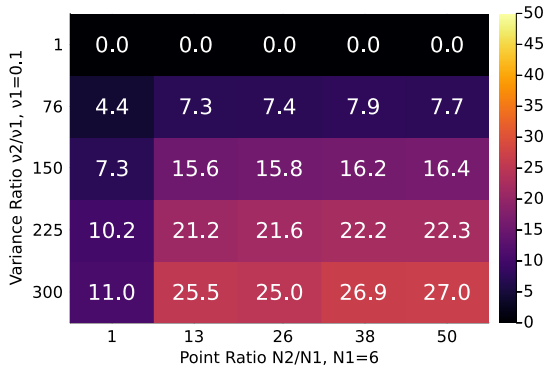
(a) KSS (TIPS) mean clustering error.

(b) ALPCAUS ($B = 1$, TIPS) mean clustering error.(c) EKSS ($B=128$) mean clustering error.(d) ALPCAUS ($B=128$) mean clustering error.

(e) TSC mean clustering error.



(f) ADSSC mean clustering error.



(g) Noisy oracle mean clustering error.

v_2/v_1	1	1	300	300	150	225	76
N_2/N_1	1	50	1	50	26	13	38
Reference Level							
Noisy Oracle	0.0	0.0	11.0	27.0	15.8	21.2	7.9
Method Comparisons							
KSS	26.6	19.9	37.8	45.6	38.9	44.4	24.8
EKSS ($B = 128$)	0.2	0.0	31.6	42.4	25.7	40.4	8.0
ADSSC	0.3	0.0	22.7	42.2	31.7	38.6	10.6
TSC	37.1	0.0	43.8	43.5	28.5	38.2	9.9
ALPCAUS ($B = 1$)	25.8	16.7	35.1	37.8	31.9	35.3	18.5
ALPCAUS ($B = 128$)	0.0	0.0	26.4	27.8	16.1	22.7	7.8

(h) Clustering error (%) results for heteroscedastic landscape. Visual results included in Fig. 2. Columns consist of the 4 corners and the 3 diagonal elements of the heatmaps in Fig. 2.

Fig. 2: Clustering error over the heteroscedastic landscape for various subspace clustering algorithms.

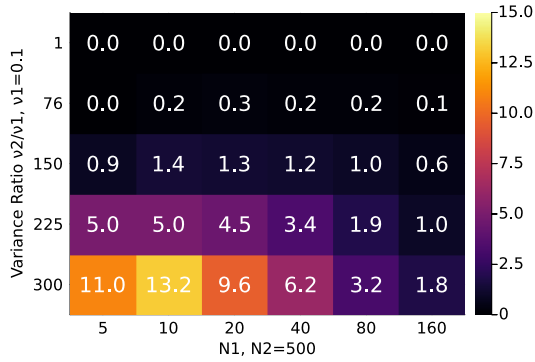


Fig. 3: Percentage difference (%) of ALPCAHUS clustering error subtracted from EKSS while good data amount varies.

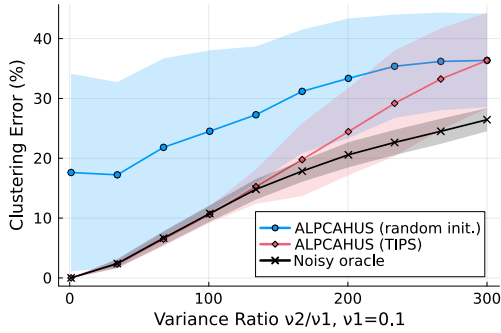


Fig. 4: Clustering error (%) for TIPS initialization scheme vs. random initialization for the ALPCAHUS method ($B = 1$).

5) *Rank Estimation of Clusters*: In Sec. IV-C, a random sign flipping method is proposed to adaptively find and shrink the subspace dimension of clusters when subspace dimension is unknown. In Fig. 5, synthetic subspaces are generated with true rank $d = 6$ to explore how the initial rank parameter affects the ability to estimate the true rank over 100 trials. This approach is compared against the eigengap heuristic by using ALPCAHUS with both adaptive rank schemes and report the estimated rank values from the final clustering. The eigengap approach consistently underestimated the rank regardless of the initial value, except when given the true rank value $d = 6$. Our sign flipping approach provided much better rank estimates with smaller variances between trials.

B. Real Data Experiments

1) *Quasar Flux Data*: Quasar spectra data is downloaded from the Sloan Digital Sky Survey (SDSS) Data Release 16 [42] using the DR16Q quasar catalog [43]. Each quasar has a vector of flux measurements across wavelengths that describes the intensity of observing that particular wavelength. In this dataset, the noise is heteroscedastic across the sample space (quasars) and feature space (wavelength), but for these experiments, we focused on a subset of data that is homoscedastic across wavelengths and heteroscedastic across quasars. The noise for each quasar is known given the measurement devices used for data collection [42]. In Fig. 7, a subset of the spectra data is shown for illustrative purposes to compare the visual differences in data quality. The preprocessing pipeline for the data included

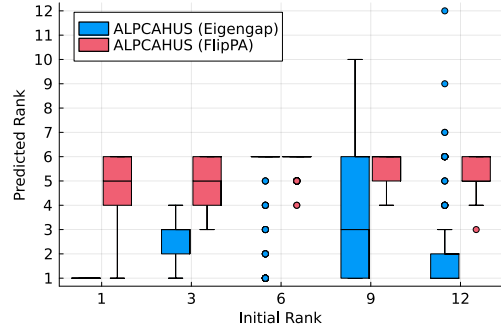
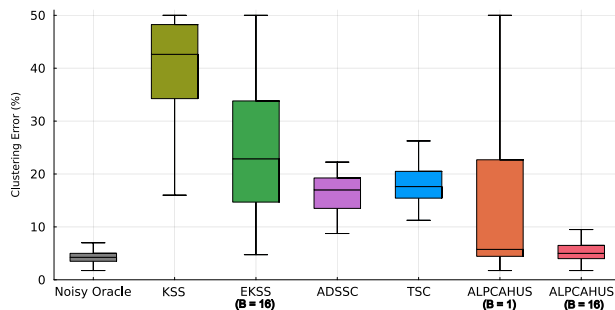


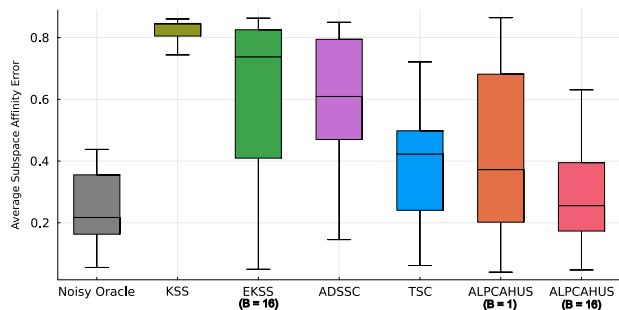
Fig. 5: Adaptive rank estimation using eigengap heuristic and proposed FlipPA approach (true rank $d = 6$).

(filtering, interpolation, centering, and normalization) based on the supplementary material of Ref. [44]. Clusters are formed in these experiments by considering quasars with different properties, namely, two quasar groups ($K = 2$) with different redshift values ($z_1 = 1.0 - 1.1$, $z_2 = 2.0 - 2.1$). Additionally, for the second group, only broad absorption lines (BAL) type quasar data is collected. Since the downloaded data is queried separately, clustering association is known, meaning one can compute clustering error for comparison purposes. A training set (5000 samples) is set aside to learn any model parameters and the rest (5000 samples) is used for a test dataset. Trials are formed by randomly selecting 400 quasar spectra samples per group and running clustering algorithms for 50 total trials. For rank estimation, the noisy oracle approach is used, given the known cluster labels, to find that there is no improvement to clustering quality for rank values greater than $\hat{d} = 3$, so this value is used for any applicable algorithms.

Fig. 6a shows clustering error for this quasar spectra multi-cluster data. The ensemble version of ALPCAHUS was very close in clustering quality to the noisy oracle, suggesting that it accurately learned the subspace bases while clustering the data groups. The non-ensemble version of ALPCAHUS ($B = 1$) had large variances in clustering error, indicating some challenges in getting close to the optimal cost function minima with this data. However, based on median values, it still managed to get a lower error than KSS, ADSSC, and TSC. Additionally, Fig. 6b shows the average subspace affinity error of these methods after applying LR-ALPCAH to the clusterings for all methods. ALPCAHUS better learned the subspace bases than the other methods when $B = 16$, which was chosen as the smallest value that had small run-to-run variances while not taking significantly longer to compute. Both of these results show the benefit of developing heteroscedastic-based algorithms in the subspace clustering context. Table I reports median time complexity and memory requirements along with mean clustering error and mean subspace error. In this quasar example, the ensemble method gets close in time to the non-ensemble methods due to our multi-threaded implementation. Yet, because of the multi-threaded implementation, the memory requirements are larger for the ensemble method as opposed to the non-ensemble method. Overall, relative to other clustering methods, ALPCAHUS is competitive time-wise at the cost of increased memory requirements.



(a) Subspace clustering results for various methods.



(b) Average subspace affinity error results for various methods.

Fig. 6: Experimental results of quasar flux data for subspace clustering and learning. Methods involving a single run, i.e., KSS and ALPCAUS ($B = 1$), use the TIPS initialization scheme.

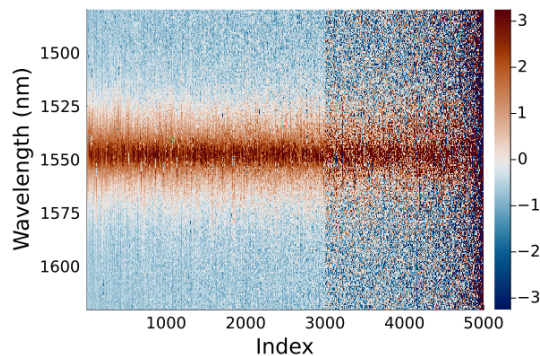


Fig. 7: Sample data matrix of quasar flux measurements across wavelengths for each column-wise sample.

2) *Indian Pines Data*: Hyperspectral image (HSI) segmentation data is explored in this section, specifically Indian Pines [45]. This image of size 145×145 contains $D = 200$ reflectance bands for each pixel that is around the $0.4 - 2.5 \mu m$ wavelength. HSI data is known to be very noisy due to thermal effects, atmospheric effects, and camera electronics, leading to works that study per-pixel noise estimation in hyperspectral imaging [46]. In total, there are $K = 16$ classes composed of alfalfa, corn, grass, wheat, soybean, and others. There is one additional class (background) that is withheld from clustering as commonly done in other works [32]. Because of this, the data contains $N = 10,249$ samples instead of $N = 145 \times 145$ samples. In other works, researchers have found that $\hat{d} = 5$ is an appropriate rank parameter since it covers 95% of the cumulative variance [32]. A subset of the data matrix $Y \in \mathbb{R}^{200 \times 10249}$ is split into 2500 samples to learn model parameters. From this, the learned subspaces are applied on Y to cluster all data so that the heatmaps can be compared against the ground truth. The ground truth image is found in Fig. 8a. For perspective, randomly guessing would lead to 94% clustering error due to $K = 16$ clusters. For consistency, the Hungarian algorithm is again applied to the clustering results in Fig. 8 to make it easier to compare against the ground truth label image in Fig. 8a.

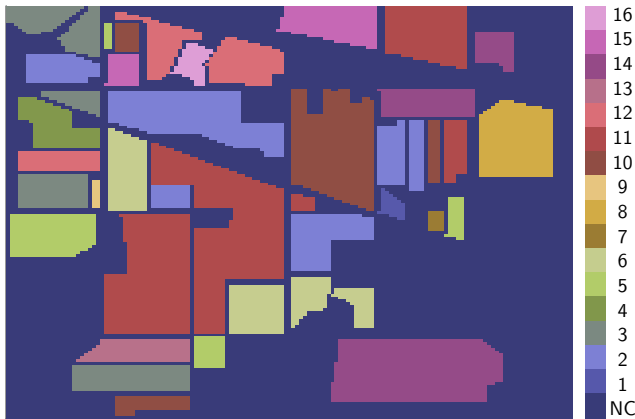
K -means is included in Fig. 8b to illustrate the difficulty of the problem. ALPCAUS results are shown in Fig. 8d next to EKSS results in Fig. 8c. Clustering error is reported for

Methods	Time (ms)	Memory (MiB)	Mean Subspace Error	Mean Clustering Error (%)
KSS	149.3	53.0	0.80	38.5
EKSS ($B=16$)	181.4	212.6	0.62	23.8
ADSSC	125.7	17.5	0.62	21.1
TSC	32.3	16.5	0.40	18.2
ALPCAUS ($B=1$)	148.5	126.7	0.43	14.4
ALPCAUS ($B=16$)	210.7	678.2	0.28	6.3

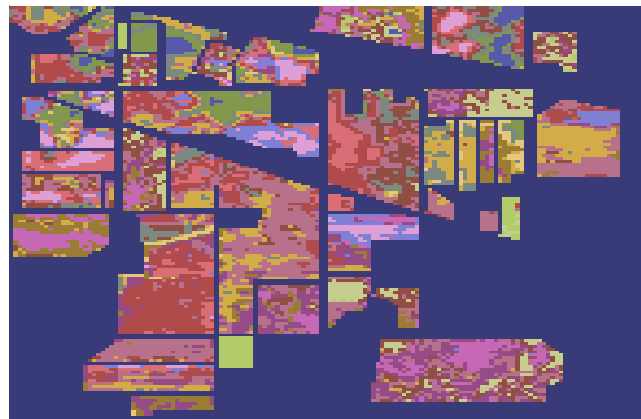
TABLE I: Subspace clustering results on quasar flux data. The KSS and ALPCAUS ($B = 1$) methods use TIPS initialization.

these algorithms along with mean intersection over union (IOU) to measure the similarity between the images. ALPCAUS achieved the lowest clustering error and highest mIOU values (53%, 31%) relative to the other approaches such as K -means (77%, 16%) and EKSS (64%, 27%). We note that our ALPCAUS results are similar to Ref. [32] even though, in that work, the authors treat the noise as homoscedastic and the signal itself as heteroscedastic. Further, the EKSS results on this dataset are similar to the homoscedastic PCA approach used in Ref. [32]. This indicates some utility in modeling heteroscedasticity in hyperspectral images. Yet, the reflectance bands themselves also appear to be heteroscedastic with some bands being noisier than others [47]. Thus, developing a method that is doubly heteroscedastic with respect to both the samples and features is an interesting direction for future work.

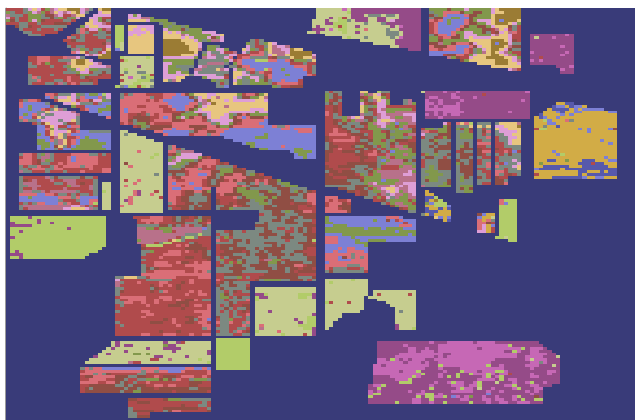
For reference, the state of the art result is about 10% misclassification rate in a *classification* setting (i.e., not clustering) [48]. In a clustering setting, recent works such as Ref. [49] have achieved a 40% clustering error which is 13% lower than our results. We do not claim state of the art results with this HSI data, only that heteroscedastic union of subspace modeling improved results over homoscedastic union of subspace modeling in finding reflectance band groups with similar characteristics.



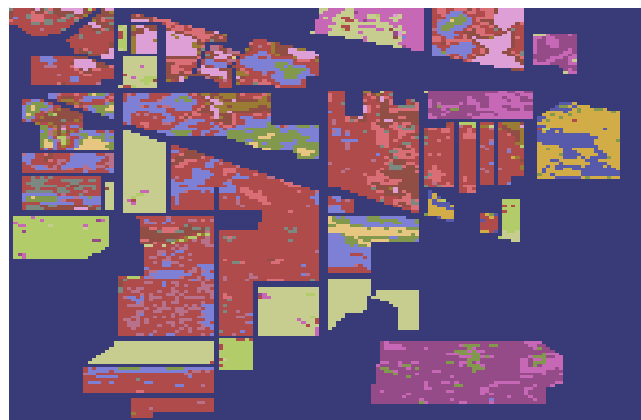
(a) Ground truth labels for *Indian Pines* dataset. NC means no class available (background).



(b) K -means results with clustering error = 77% and mIOU = 16%.



(c) EKSS ($B = 32, T = 3, q = K$) results with clustering error = 64% and mIOU = 27%.



(d) ALPCHUS ($B = 32, T = 3, q = K$) results with clustering error = 53% and mIOU = 31%.

Fig. 8: Experimental results of *Indian Pines* HSI data in a subspace clustering context. Results reported are clustering error and mean IOU (intersection over union) for each algorithm.

VI. CONCLUSION

This paper proposed ALPCHUS, a subspace clustering algorithm that can find subspace clusters whose samples contain heteroscedastic noise. For future work, a union of manifolds generalization by deep learning could be useful. For example, Alzheimer’s disease patients often have resting state functional MRI activations different than cognitively normal individuals [50], so one could consider these different classes to belong to different manifolds in the ambient space. Previous research has shown manifold learning to more correctly model temporal dynamics as opposed to subspace modeling in this domain [51]. Another direction of future work could be to consider heteroscedasticity across the feature space instead of the sample space. For example, one might be interested in biological sequencing of different species with similar genes where the gene marker counts naturally follow heteroscedastic distributions [52]. Another interesting topic would be to explore Thm. 1 in greater detail. This theorem simply states that ALPCHUS generates a sequence of cost function values that converge; it says nothing about recovery guarantees or the quality of that

solution. Thus, provably showing how the basin of attraction changes as heteroscedastic data is introduced would lead to a greater understanding of heteroscedasticity in a subspace clustering context. Additionally, per Sec. VIII-B, extending the method to handle extremely imbalanced cluster sizes would be another interesting avenue. These generalizations are nontrivial so they are left for future work.

While our implementation of ALPCHUS benefited from parallelization, it needed more computation time and memory than TSC. Because of this, there is an opportunity to further optimize our code base to remove certain matrix multiplication operations and instead use single vector dot products to reduce memory. Further, since our subspace basis step requires an SVD computation for an initial low-rank estimate, perhaps the Krylov-based Lanczos algorithm [53] can be used to further reduce time and memory for each trial leading to more significant improvements in memory usage and time. These additions can be fruitful in big data settings. Overall, ALPCHUS was more robust towards heteroscedastic noise than other clustering methods, making it easier to identify correct clusterings under this kind of heterogeneity model.

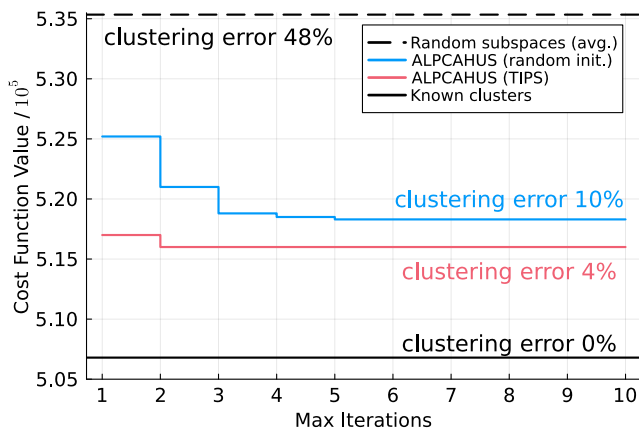


Fig. 9: ALPCAUS ($B = 1$) cost function value convergence plot to corroborate the theorem in Thm. 1.

VII. ACKNOWLEDGMENTS

This work was supported in part by the National Science Foundation (NSF) under NSF CAREER Grant CCF-1845076, NSF Grant CCF-2331590, and by the U.S. National Institutes of Health (NIH) under Grant R21 AG082204. We thank David Hong for suggesting heteroscedastic data applications such as astronomy spectra that is used in this work.

VIII. APPENDIX

A. ALPCAUS Convergence Experiment

This section focuses on providing empirical verification of the ALPCAUS convergence theorem in Thm. 1. The quasar spectra flux data from SDSS (DR16Q catalog) is used in this experiment. The noise variance threshold parameter α is set to 10^{-6} to lower bound the noise variance estimation. Further, as shown in Thm. 1, it is necessary to use the cluster reassignment criteria in (27) that rejects repeated assignments of points to prevent cycling. For simplicity, only one base clustering ($B = 1$) is used in this experiment to compare a randomly initialized ALPCAUS trial against the TIPS initialized variant. This variant is only possible when $B = 1$ as discussed in the paper. In Fig. 9, the cost function value is plotted over iterations for both versions of ALPCAUS.

Both upper and lower bound cost function reference values are provided in Fig. 9. The upper bound is generated by using randomly initialized subspaces, and by applying (27) to get cluster labels. From this, the cost function value is computed by (19). Likewise, a lower bound is generated by using the known cluster labels, and by estimating the subspaces and noise variances by (20). As observed in Fig. 9, ALPCAUS converges relatively quickly with only a few iterations. Note that in this figure, the stopping criteria in line (10) of Alg. ALPCAUS is purposely ignored. In other words, ALPCAUS is run for a fixed number of iterations. However, as clearly demonstrated, convergence is achieved earlier for both versions of ALPCAUS before reaching the maximum number of iterations. This indicates the usefulness of the stopping criteria to speed up the algorithm in various applications.

B. Balanced Cluster Assumption

The ensemble extension of ALPCAUS relies on forming an affinity matrix in (28) that is thresholded by (29) and (30). Then, spectral clustering is applied on said affinity matrix which depends on (4). This spectral clustering operation, by the normalized cut function in (4), assumes balanced cluster partitions to avoid trivial solutions such as finding a small cut that leads to a single point belonging to its own cluster and everything else being in another cluster. Thus, the proposed ALPCAUS method may not be ideal in situations where imbalanced clusters exist.

While one could use other clustering methods for imbalanced data such as Ref. [54] or Ref. [55], these methods are not ideal in heterogeneous settings as they do not account for heteroscedasticity in the data. Instead, we recommend using the partition cut (“Pcut”) method introduced in Ref. [56] that performs spectral clustering-like operations on a rank-modulated degree graph as a replacement for spectral clustering which uses the normalized cut function (“Ncut”) in (4). This would allow for ALPCAUS to be more robust towards imbalanced cluster size situations. Furthermore, the non-ensemble version of ALPCAUS in (19), may also suffer in the imbalanced cluster regime if the TIPS-based initialization scheme in Sec. IV-D is used. This is due to the spectral clustering operation in TIPS to initialize cluster labels for ALPCAUS. Therefore, even when $B = 1$, it is also recommended to apply the “Pcut” method in Ref. [56] on the affinity matrix formed by (39).

C. ALPCAUS Parameters

For Alg. ALPCAUS, the input data matrix $Y \in \mathbb{R}^{D \times N}$ and the number of subspaces/clusters $K \in \mathbb{Z}^+$ are necessary inputs that are clearly data dependent. For the candidate subspace dimension \hat{d}_k , it may be the same across all clusters or vary, and it is either known via domain knowledge or can be reasonably estimated by the procedure outlined in Sec. IV-C. If it must be estimated, it is recommended to start over-parameterized rather than under-parameterized. A scree plot of Y can give an indication of sufficient rank for initialization to ensure an over-parameterized state. Further, \hat{d}_k may also be treated simply as a hyperparameter for cross validation purposes.

For the threshold parameter $q \in \mathbb{Z}^+$, this can be set to the subspace dimension as shown in Ref. [36] and explained in Sec. IV-A, or simply treated as a hyperparameter to be optimized during cross validation; this value is dataset dependent. The number of base clusterings $B \in \mathbb{Z}^+$ is either fixed to $B = 1$ for the non-ensemble version of ALPCAUS, or set as high as compute time and memory allows for the ensemble version. In other words, more trials make it easier to identify the underlying relationships between similar data samples. If $B = 1$, then it is recommended to use the TIPS-based initialization scheme from Sec. IV-D.

Since each subspace basis update involves LR-ALPCAUS [17], the $T_1 \in \mathbb{Z}^+$ parameter specifies the number of LR-ALPCAUS iterations. For T_1 , it is recommended to keep some low value, e.g., we set $T_1 = 5$ since there is no point in converging perfectly as the cluster labels will get updated

in the next reassignment anyway at the $t_2 + 1$ iteration. For the non-ensemble version, it is recommended to do as many alternating updates $T_2 \in \mathbb{Z}^+$ as necessary to trigger the stopping criteria in line (10) of Alg. ALPCAUS. However, for the ensemble version of ALPCAUS, we find that a low value such as $T_2 = 3$ works very well in practice due to the larger number of trials $B \gg 1$. This value agrees with Fig. 9 as ALPCAUS converges in just a few iterations anyway. For more detailed and practical code-oriented function usage, refer to the documentation at github.com/javieresc1/ALPCAUS.

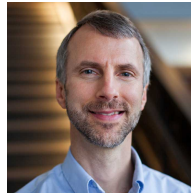
REFERENCES

- [1] Y. Chen, Y. Tang, C. Wang, X. Liu, L. Zhao, and Z. Wang, "ADHD classification by dual subspace learning using resting-state functional connectivity," *Artificial intelligence in medicine*, vol. 103, p. 101786, 2020.
- [2] Q. Jia, J. Cai, X. Jiang, and S. Li, "A subspace ensemble regression model based slow feature for soft sensing application," *Chinese Journal of Chemical Engineering*, vol. 28, no. 12, pp. 3061–3069, 2020.
- [3] W. He, N. Yokoya, and X. Yuan, "Fast hyperspectral image recovery of dual-camera compressive hyperspectral imaging via non-iterative subspace-based fusion," *IEEE Transactions on Image Processing*, vol. 30, pp. 7170–7183, 2021.
- [4] R. Vidal, "Subspace clustering," *IEEE Signal Processing Magazine*, vol. 28, no. 2, pp. 52–68, 2011.
- [5] A. Y. Yang, J. Wright, Y. Ma, and S. S. Sastry, "Unsupervised segmentation of natural images via lossy data compression," *Computer Vision and Image Understanding*, vol. 110, no. 2, pp. 212–225, 2008.
- [6] R. Vidal, R. Tron, and R. Hartley, "Multiframe motion segmentation with missing data using PowerFactorization and GPCA," *International Journal of Computer Vision*, vol. 79, pp. 85–105, 2008.
- [7] W. Hong, J. Wright, K. Huang, and Y. Ma, "Multiscale hybrid linear models for lossy image representation," *IEEE Transactions on Image Processing*, vol. 15, no. 12, pp. 3655–3671, 2006.
- [8] R. Vidal, S. Soatto, Y. Ma, and S. Sastry, "An algebraic geometric approach to the identification of a class of linear hybrid systems," in *42nd IEEE International Conference on Decision and Control (IEEE Cat. No. 03CH37475)*, vol. 1. IEEE, 2003, pp. 167–172.
- [9] [Online]. Available: <https://www.epa.gov/outdoor-air-quality-data>
- [10] P. Tsalmantza and D. W. Hogg, "A data-driven model for spectra: Finding double redshifts in the sloan digital sky survey," *The Astrophysical Journal*, vol. 753, no. 2, p. 122, 2012.
- [11] Y. Cao, A. Zhang, and H. Li, "Multisample estimation of bacterial composition matrices in metagenomics data," *Biometrika*, vol. 107, no. 1, pp. 75–92, 12 2019. [Online]. Available: <https://doi.org/10.1093/biomet/asz062>
- [12] D. Hong, L. Balzano, and J. A. Fessler, "Asymptotic performance of PCA for high-dimensional heteroscedastic data," *J. Multivar. Anal.*, vol. 167, no. C, p. 435–452, sep 2018. [Online]. Available: <https://doi.org/10.1016/j.jmva.2018.06.002>
- [13] E. Elhamifar and R. Vidal, "Sparse subspace clustering: Algorithm, theory, and applications," *IEEE transactions on pattern analysis and machine intelligence*, vol. 35, no. 11, pp. 2765–2781, 2013.
- [14] P. K. Agarwal and N. H. Mustafa, "K-means projective clustering," in *Proceedings of the twenty-third ACM SIGMOD-SIGACT-SIGART symposium on Principles of database systems*, 2004, pp. 155–165.
- [15] R. Heckel and H. Bölcskei, "Robust subspace clustering via thresholding," *IEEE Transactions on Information Theory*, vol. 61, no. 11, pp. 6320–6342, 2015.
- [16] J. Lipor, D. Hong, Y. S. Tan, and L. Balzano, "Subspace clustering using ensembles of k-subspaces," *Information and Inference: A Journal of the IMA*, vol. 10, no. 1, pp. 73–107, 2021.
- [17] J. Salazar Cavazos, J. A. Fessler, and L. Balzano, "ALPCAUS: Subspace learning for sample-wise heteroscedastic data," *Transactions on Signal Processing (TSP)*, pp. 1–12, 2025.
- [18] J. P. Costeira and T. Kanade, "A multibody factorization method for independently moving objects," *International Journal of Computer Vision*, vol. 29, pp. 159–179, 1998.
- [19] L. Lu and R. Vidal, "Combined central and subspace clustering for computer vision applications," in *Proceedings of the 23rd international conference on Machine learning*, 2006, pp. 593–600.
- [20] S. R. Rao, R. Tron, R. Vidal, and Y. Ma, "Motion segmentation via robust subspace separation in the presence of outlying, incomplete, or corrupted trajectories," in *2008 IEEE conference on computer vision and pattern recognition*. IEEE, 2008, pp. 1–8.
- [21] A. Ng, M. Jordan, and Y. Weiss, "On spectral clustering: Analysis and an algorithm," *Advances in neural information processing systems*, vol. 14, 2001.
- [22] F. Nie, Z. Zeng, I. W. Tsang, D. Xu, and C. Zhang, "Spectral embedded clustering: A framework for in-sample and out-of-sample spectral clustering," *IEEE Transactions on Neural Networks*, vol. 22, no. 11, pp. 1796–1808, 2011.
- [23] W. Qu, X. Xiu, H. Chen, and L. Kong, "A survey on high-dimensional subspace clustering," *Mathematics*, vol. 11, no. 2, p. 436, 2023.
- [24] R. Vidal and P. Favaro, "Low rank subspace clustering (LRSC)," *Pattern Recognition Letters*, vol. 43, pp. 47–61, 2014.
- [25] P. S. Bradley and O. L. Mangasarian, "K-plane clustering," *Journal of Global optimization*, vol. 16, pp. 23–32, 2000.
- [26] P. Wang, H. Liu, A. M.-C. So, and L. Balzano, "Convergence and recovery guarantees of the k-subspaces method for subspace clustering," in *International Conference on Machine Learning*. PMLR, 2022, pp. 22 884–22 918.
- [27] A. Gitlin, B. Tao, L. Balzano, and J. Lipor, "Improving k-subspaces via coherence pursuit," *IEEE Journal of Selected Topics in Signal Processing*, vol. 12, no. 6, pp. 1575–1588, 2018.
- [28] M. E. Timmerman, E. Ceulemans, K. De Roover, and K. Van Leeuwen, "Subspace k-means clustering," *Behavior research methods*, vol. 45, pp. 1011–1023, 2013.
- [29] J. Ghosh and A. Acharya, "Cluster ensembles," *Wiley interdisciplinary reviews: Data mining and knowledge discovery*, vol. 1, no. 4, pp. 305–315, 2011.
- [30] D. Hong, K. Gilman, L. Balzano, and J. A. Fessler, "HePPCAT: Probabilistic PCA for data with heteroscedastic noise," *IEEE Transactions on Signal Processing*, vol. 69, pp. 4819–4834, 2021.
- [31] A. R. Zhang, T. T. Cai, and Y. Wu, "Heteroskedastic PCA: Algorithm, optimality, and applications," *The Annals of Statistics*, vol. 50, no. 1, pp. 53–80, 2022.
- [32] A. Collas, F. Bouchard, A. Breloy, G. Ginolhac, C. Ren, and J.-P. Ovarlez, "Probabilistic pca from heteroscedastic signals: geometric framework and application to clustering," *IEEE Transactions on Signal Processing*, vol. 69, pp. 6546–6560, 2021.
- [33] R. A. Lobos, J. Salazar Cavazos, R. R. Nadakuditi, and J. A. Fessler, "Smooth optimization algorithms for global and locally low-rank regularizers," *arXiv preprint arXiv:2505.06073*, 2025.
- [34] J. Salazar Cavazos, J. A. Fessler, and L. Balzano, "ALPCAUS: Sample-wise heteroscedastic PCA with tail singular value regularization," in *2023 International Conference on Sampling Theory and Applications (SampTA)*. IEEE, 2023, pp. 1–6.
- [35] Y. Chi, Y. M. Lu, and Y. Chen, "Nonconvex optimization meets low-rank matrix factorization: An overview," *IEEE Transactions on Signal Processing*, vol. 67, no. 20, pp. 5239–5269, 2019.
- [36] X. Peng, Z. Yu, Z. Yi, and H. Tang, "Constructing the l2-graph for robust subspace learning and subspace clustering," *IEEE transactions on cybernetics*, vol. 47, no. 4, pp. 1053–1066, 2016.
- [37] D. Hong, Y. Sheng, and E. Dobriban, "Selecting the number of components in PCA via random signflips," 2023.
- [38] M. Wright, "Speeding up the hungarian algorithm," *Computers & Operations Research*, vol. 17, no. 1, pp. 95–96, 1990.
- [39] R. Heckel and H. Bölcskei, "Robust subspace clustering via thresholding," *IEEE Transactions on Information Theory*, vol. 61, no. 11, pp. 6320–6342, 2015.
- [40] T. Ding, D. Lim, R. Vidal, and B. D. Haeffele, "Understanding doubly stochastic clustering," in *International Conference on Machine Learning*. PMLR, 2022, pp. 5153–5165.
- [41] M. Ahmed, R. Seraj, and S. M. S. Islam, "The k-means algorithm: A comprehensive survey and performance evaluation," *Electronics*, vol. 9, no. 8, p. 1295, 2020.
- [42] R. Ahumada, C. A. Prieto, A. Almeida, F. Anders, S. F. Anderson, B. H. Andrews, B. Anguiano, R. Arcodia, E. Armengaud, M. Aubert *et al.*, "The 16th data release of the sloan digital sky surveys: first release from the apogee-2 southern survey and full release of eboss spectra," *The Astrophysical Journal Supplement Series*, vol. 249, no. 1, p. 3, 2020.
- [43] B. W. Lyke, A. N. Higley, J. McLane, D. P. Schurhammer, A. D. Myers, A. J. Ross, K. Dawson, S. Chabanier, P. Martini, H. D. M. Des Bourbonx *et al.*, "The sloan digital sky survey quasar catalog: Sixteenth data release," *The Astrophysical Journal Supplement Series*, vol. 250, no. 1, p. 8, 2020.

- [44] D. Hong, F. Yang, J. A. Fessler, and L. Balzano, "Optimally weighted PCA for high-dimensional heteroscedastic data," *SIAM Journal on Mathematics of Data Science*, vol. 5, no. 1, pp. 222–250, 2023.
- [45] M. F. Baumgardner, L. L. Biehl, and D. A. Landgrebe, "220 band aviris hyperspectral image data set: June 12, 1992 indian pine test site 3," Sep 2015. [Online]. Available: <https://purrr.purdue.edu/publications/1947/1>
- [46] A. Mahmood and M. Sears, "Per-pixel noise estimation in hyperspectral images," *IEEE Geoscience and Remote Sensing Letters*, vol. 19, pp. 1–5, 2021.
- [47] S. Zhang, X. Kang, Y. Mo, and S. Li, "Noise analysis of hyperspectral images captured by different sensors," in *IGARSS 2020-2020 IEEE International Geoscience and Remote Sensing Symposium*. IEEE, 2020, pp. 2707–2710.
- [48] D. Uchaev and D. Uchaev, "Small sample hyperspectral image classification based on the random patches network and recursive filtering," *Sensors*, vol. 23, no. 5, p. 2499, 2023.
- [49] S. Huang, H. Zhang, Q. Du, and A. Pivovurica, "Sketch-based subspace clustering of hyperspectral images," *Remote Sensing*, vol. 12, no. 5, p. 775, 2020.
- [50] R. Sperling, "The potential of functional MRI as a biomarker in early alzheimer's disease," *Neurobiology of aging*, vol. 32, pp. S37–S43, 2011.
- [51] J.-H. Kim, Y. Zhang, K. Han, Z. Wen, M. Choi, and Z. Liu, "Representation learning of resting state fmri with variational autoencoder," *NeuroImage*, vol. 241, p. 118423, 2021.
- [52] R. K. Gupta and J. Kuznicki, "Biological and medical importance of cellular heterogeneity deciphered by single-cell rna sequencing," *Cells*, vol. 9, no. 8, p. 1751, 2020.
- [53] R. M. Larsen, "Lanczos bidiagonalization with partial reorthogonalization," *DAIMI Report Series*, no. 537, 1998.
- [54] J. Salazar Cavazos, "PET-TURTLE: Deep unsupervised support vector machines for imbalanced data clusters," *IEEE Signal Processing Letters*, vol. 33, pp. 91–95, 2026.
- [55] C. You, C. Li, D. P. Robinson, and R. Vidal, "Scalable exemplar-based subspace clustering on class-imbalanced data," in *Proceedings of the European Conference on Computer Vision (ECCV)*, September 2018.
- [56] J. Qian and V. Saligrama, "Spectral clustering with imbalanced data," in *2014 IEEE International Conference on Acoustics, Speech and Signal Processing (ICASSP)*. IEEE, 2014, pp. 3057–3061.



include signal and image processing, machine learning, deep learning, and optimization. Current work focuses on topics such as low-rank modeling, clustering, noisy data, and Alzheimer's disease diagnosis and prediction from functional MRI data.



Jeffrey A. Fessler (Fellow, IEEE) received the B.S.E.E. degree from Purdue University, West Lafayette, IN, USA, in 1985, the M.S.E.E. degree from Stanford University, Stanford, CA, USA, in 1986, and the M.S. degree in statistics and the Ph.D. degree in electrical engineering from Stanford University, in 1989 and 1990, respectively. From 1985 to 1988, he was a National Science Foundation Graduate Fellow with Stanford. Currently, he is the William L. Root Distinguished University Professor of EECS with the University of Michigan, Ann Arbor, MI, USA. His research focuses on various aspects of imaging problems, and he has supervised doctoral research in PET, SPECT, X-ray CT, MRI, and optical imaging problems. In 2006, he became a fellow of the IEEE for contributions to the theory and practice of image reconstruction.



Laura Balzano (Senior Member, IEEE) received the Ph.D. degree in ECE from the University of Wisconsin, Madison, WI, USA. Currently, she is an Associate Professor of electrical engineering and computer science with the University of Michigan, Ann Arbor, MI, USA. Her main research focuses on modeling and optimization with big, messy data – highly incomplete or corrupted data, uncalibrated data, and heterogeneous data – and its applications in a wide range of scientific problems. She is an Associate Editor for IEEE Open Journal of Signal Processing and SIAM Journal of the Mathematics of Data Science. She was a recipient of the NSF Career Award, the ARO Young Investigator Award, and the AFOSR Young Investigator Award. She was also a recipient of the Sarah Goddard Power Award at the University of Michigan.